

# Highly efficient hydrogenation of cinnamaldehyde to 3-phenylpropanol on Ni/NiS-modified twin Zn<sub>0.5</sub>Cd<sub>0.5</sub>S under visible light

Yujia Hu,<sup>a</sup> Guiyang Yu,<sup>\*b,c</sup> Shanshan Liu,<sup>a</sup> Chenyang Zhao,<sup>b</sup> Jianzhuang Jiang<sup>\*d</sup> and Xiyou Li<sup>\*b,e</sup>

a. College of chemistry and chemical engineering, China University of Petroleum (East China), Qingdao, 266580, China.

b. School of Materials Science and Engineering, China University of Petroleum (East China), Qingdao, 266580, China.

E-mail: xiyouli@upc.edu.cn. yuguizhang333@163.com

c. Key Laboratory of Eco-chemical Engineering, Qingdao University of Science and Technology, Qingdao 266042, P. R. China.

d. Beijing Key Laboratory for Science and Application of Functional Molecular and Crystalline Materials, Department of Chemistry, University of Science and Technology Beijing, Beijing 100083, China.

E-mail: jianzhuang@ustb.edu.cn

e. Key Laboratory of Heavy Oil Processing, Institute of New Energy, China University of Petroleum (East China), Qingdao, 266580, China.

# Contents

## Experimental Section

**Fig. S1.** Zeta potentials of the ZCS suspension solution.

**Fig. S2.** (a) HRTEM image and (b) EDS spectra of 0.5% Ni/NiS-ZCS sample.

**Fig. S3.** XRD patterns of as-prepared NiS sample.

**Fig. S4.** N<sub>2</sub> absorption-desorption isotherms (inset: the corresponding BET surface area) of ZCS and Ni/NiS-ZCS samples.

**Fig. S5.** (a) XPS full spectra survey and (b) S 2p XPS spectra of ZCS and 0.5% Ni/NiS-ZCS samples.

**Fig. S6.** The peak areas for the known product concentrations were used to generate a calibration curve of (a) CAL, (b) HCOL and (c) COL.

**Fig. S7.** The effect of reaction temperature on the photocatalytic performance upon Ni/NiS-ZCS sample at two temperatures with 277 K and 290 K.

**Fig. S8.** The conversion efficiency of CAL in different (a) solvent composition and (b) volume ratio of ethanol/water system using ZCS as photocatalyst. (c) Bar chart of HCOL yield for 1 h reaction time over ZCS photocatalyst.

**Fig. S9.** XRD patterns of fresh and used 0.5% Ni/NiS-ZCS samples.

**Fig. S10.** UV-vis spectra of fresh and used 0.5% Ni/NiS-ZCS samples.

**Fig. S11.** (a) Cd 3d, (b) Zn 2p and (c) Ni 2p XPS spectra of fresh and used 0.5% Ni/NiS-ZCS samples.

**Fig. S12.** TEM images of fresh and used 0.5% Ni/NiS-ZCS samples.

**Fig. S13.** The cyclic voltammetry of CAL.

**Fig. S14.** UV-Vis diffuse reflectance spectra of ZCS and Ni/NiS-ZCS samples.

**Fig. S15.** (a) HCOL yield with the reaction time for Ni/NiS-ZCS and NiS-ZCS Mix samples. (b) Bar chart of HCOL yield for 1 h reaction time over Ni/NiS-ZCS and NiS-ZCS Mix samples.

**Fig. S16.** Fluorescence lifetime of ZCS and 0.5% Ni/NiS-ZCS samples.

**Fig. S17.** Mass spectra of standard HCOL in ethanol-water (7:3) solvent.

**Fig. S18.** Mass spectrometry test results of reaction products under (a) ethanol-water and (b) ethanol-D<sub>2</sub>O solvent.

**Fig. S19.** Photocatalytic activity of hydrogen evolution and HCOL yield with 0.5% Ni/NiS-ZCS (20 mg) photocatalyst under visible light irradiation.

**Fig. S20.** Liquid-phase EPR spin-trapping experiment containing Ni/NiS-ZCS photocatalyst, ethanol/H<sub>2</sub>O solvent, CAL reactant, and DMPO radical trapping agent in air.

**Fig. S21.** EPR spectra of DMPO-•OH adducts containing Ni/NiS-ZCS photocatalyst, ethanol/H<sub>2</sub>O solvent, CAL reactant, and DMPO radical trapping agent in N<sub>2</sub> atmosphere.

**Fig. S22.** Results of acetaldehyde detection in HPLC.

**Table S1.** The corresponding atomic content of different catalysts based on ICP-AES.

**Table S2.** Photocatalytic reduction of CAL to HCOL under different solvent composition.

**Table S3.** Summary of photocatalysts reported for CAL reduction.

**Table S4.** The absolute fluorescence quantum yield (%) and fluorescence lifetime of

samples excited at 380 nm in the wavelength range of 400-750 nm.

**Table S5.** Black experiments without catalyst nor light irradiation.

**Table S6. ICP results of the supernatant after centrifugation of the catalyst in the system before and after the reaction.**

**References**

## **Experiment section**

### **Materials**

Zinc acetate, cadmium acetate, thioacetamide, sodium hydroxide and nickel chloride hexahydrate were all purchased from Sinopharm Chemical Reagent Co. Ltd. Ethanol, acetonitrile were all purchased from Fuyu Chemical.

### **Synthesis of $Zn_{0.5}Cd_{0.5}S$ (ZCS)**

The detail of synthesis of  $Zn_{0.5}Cd_{0.5}S$  (ZCS) photocatalysts were described in previous work of research group.

### **Synthesis of Ni/NiS-ZCS**

Ni/NiS-ZCS was synthesized by light deposition method. Appropriate  $NiCl_2 \cdot 6H_2O$  and ZCS were mixed in 100 mL ethanol solution. Under 300 W Xenon lamp (Beijing Perfectlight Technology Co., Ltd., PLS-SXE 300D), irradiated with visible light source ( $>420$  nm). The temperature of the system was maintained within the range of 293-303 K with circulating condensate water and stirred for 5 hours. Finally, Ni/NiS-ZCS were collected by centrifuging and dried at 333 K for 8 h. The as-prepared hybrids were noted as x% Ni/NiS-ZCS, where x stands for atomic ratio of Ni element to ZCS. For instance, the atomic ratio of Ni to ZCS was 0.5 wt% for 0.5% Ni/NiS-ZCS.

### **Photocatalytic reduction of CAL to HCOL**

Typically, 20 mg catalyst and 0.1 mmol CAL were added to a photocatalytic quartz reactor containing 100 mL solvent with a capacity of 250 mL, and the suspension was

fully stirred at a constant rate. The system was bubbles degassed with argon gas for 30 min to remove oxygen in the system, and the temperature of the reaction solution was controlled at room temperature with circulating condensate water. Then 300 W xenon lamp ((Beijing Perfectlight Technology Co., Ltd., PLS-SXE 300D) equipped with 420 nm cut-off filter was selected as visible light source. After the reaction, the obtained mixture was filtered through a 0.22  $\mu\text{m}$  Nylon syringe filter, and then analyzed by high-performance liquid chromatography (HPLC). The HPLC (Shimadzu, LC-20A) is equipped with a C18 column ( $250 \times 4.6$  mm i.d., 5.0  $\mu\text{m}$ ), a LC-20A pump, and SPD-20A UV detector. The moving phase consisted of methanol: acetonitrile: water (28.4:18:53.6) with a flow rate of 1.0 mL  $\text{min}^{-1}$  and was detected at 204 nm.

### **Characterization**

The crystallographic structures of Ni/NiS-ZCS samples were analyzed by Powder X-ray diffraction (PXRD) measurements were carried out by using a Rigaka Ultima IV diffractometer with Cu Ka radiation (1.538Å). The crystallite size of the samples can be calculated by X-ray line broadening analysis according to the Scherrer formula. Scanning electron microscopy (SEM) images were recorded by using a JEOL JSM-6700F microscope at an accelerating voltage of 5 kV. The elemental analysis was carried out on an inductively coupled plasma mass spectrometry (ICP-MS, PerkinElmer, ELAN9000). The UV-vis-NIR diffuse reflectance spectra (DRS) were obtained in the range from 1800 to 300 nm using a Hitachi UH-4150 spectrophotometer with an integrated sphere attachment and  $\text{BaSO}_4$  used as the reference sample. Transmission electron microscopy (TEM) and high-resolution transmission electron

microscopy (HRTEM) images were performed with JEM 2100 instrument with an accelerating voltage of 200 kV. The Brunauer–Emmett–Teller (BET) specific surface area and pore size distribution were derived from the N<sub>2</sub> adsorption and desorption on a Beckman Coulter SA3100 analyzer at 77 K. The pretreatments of the samples were degassed under vacuum at 373 K. X-ray photoelectron spectroscopy (XPS) was carried out by using a Thermo Escalab 250 Xi using Mg K $\alpha$  as the excitation source. The high-performance liquid chromatography (HPLC, Shimadzu LC-20A, column oven CTO-20A, pump LC-20A, UV detector SPD-20A, autosampler). The column for HPLC measurement was a Shim-pack GIST C18 (250×4.6 mm I.D., 5 $\mu$ m). The column oven was kept at 308 K. The injected sample (either 1  $\mu$ l in volume) was eluted with acetonitrile-water-methanol (18:53.6:28.4) aqueous solution at a fixed flow rate (1 mL/min). The UV detector was set at 204 nm so that the absorption due to reactants and products can be easily detected. The Zeta potential test is through a Zeta potential meter. At room temperature, disperse ZCS in water to take the supernatant, and take the average value of three cycles as the zeta potential value.

### **Photocatalytic reaction**

Apparent quantum efficiencies (AQEs) were measured using different band-pass filters and an irradiation meter and were defined by the equation: <sup>[1]</sup>

$$\text{AQE} = \frac{N_E}{N_P} \times 100\% = \frac{4N_{\text{CAL}}}{N_P} \times 100\% \quad (1)$$

where N<sub>E</sub> is the number of reacted electrons, N<sub>P</sub> is the number of incident photons and N<sub>CAL</sub> is the number of evolved Cinnamaldehyde molecules.

## Photoelectrochemical measurement

The transient photocurrent responses and electrochemical impedance spectra (EIS) were measured by a CHI760D electrochemical workstation (Shanghai Chenhua Instrument Corp., China) in a three-electrode system, which consists of a working electrode, a saturated calomel reference electrode and a platinum electrode. The sample (5 mg) were dispersed in 2 mL ethanol by 2 hours ultrasonic treatment to get a slurry. Drop the mixture onto the precleaned fluoride tin oxide (FTO) glass slide and dry it on a heating table at 333 K to prepare the working electrode. The 3 electrodes were immersed in 0.5 M Na<sub>2</sub>SO<sub>4</sub> aqueous solution. During the measurement, a 300 W Xe lamp attached with a 420 nm cut-off optical filter was used to illuminate working electrode. The EIS was conducted in a frequency range from 0.01 to 10<sup>5</sup> Hz with an AC amplitude of 5 mV at 0.43 V. Cyclic voltammetry (CV) was carried out by sweeping at 0.1 V·s<sup>-1</sup> in CH<sub>3</sub>CN, which include 0.1 mol/L LiClO<sub>4</sub> and 0.2 mmol/L CAL. A Platinum carbon electrode, a platinum wire, and an Ag/AgNO<sub>3</sub> electrode (0.01 mol/L in CH<sub>3</sub>CN) were used as the working, counter, and reference electrodes, respectively.



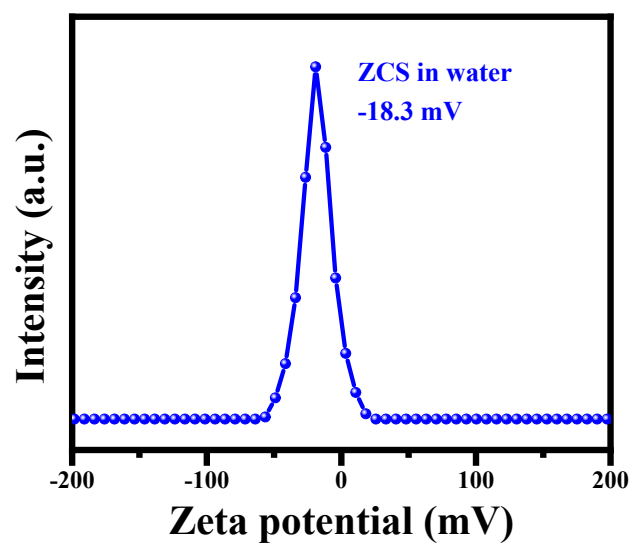


**Fig. S1.** Zeta potentials of the ZCS suspension solution.

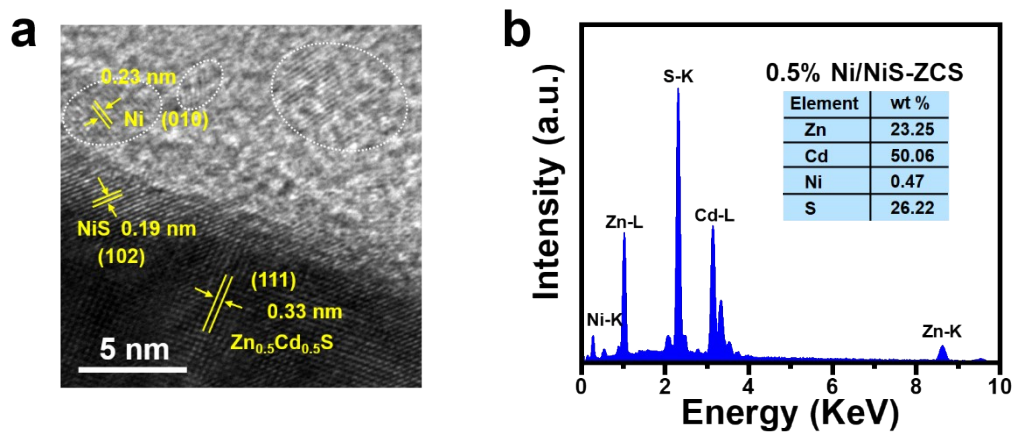


**Fig. S2.** (a) HRTEM image and (b) EDS spectra of 0.5% Ni/NiS-ZCS sample.

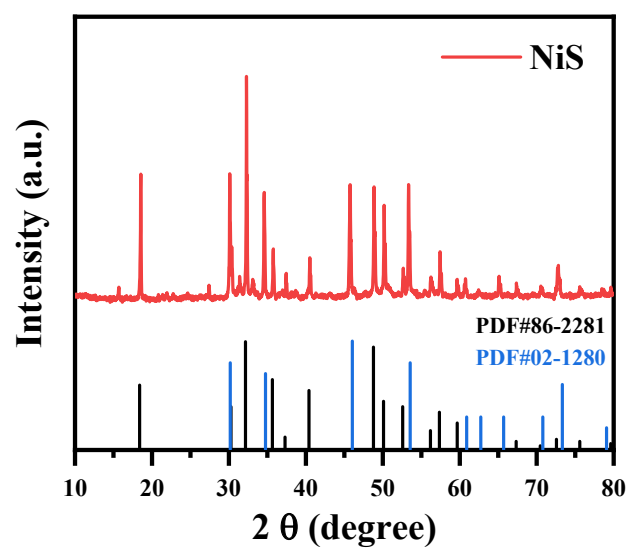
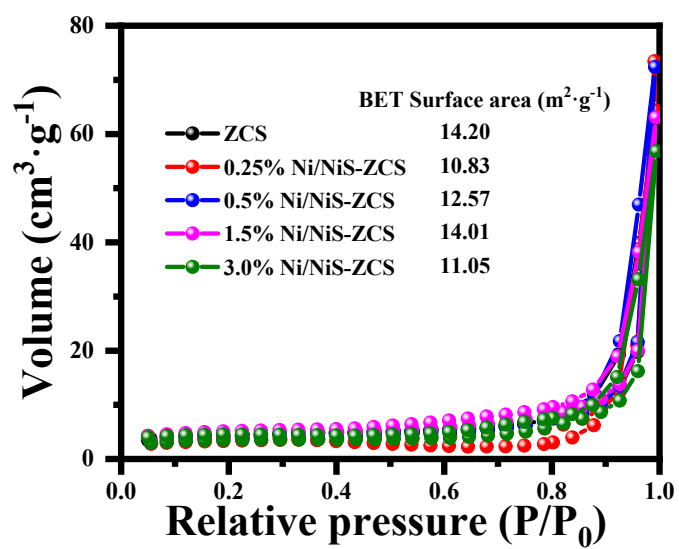
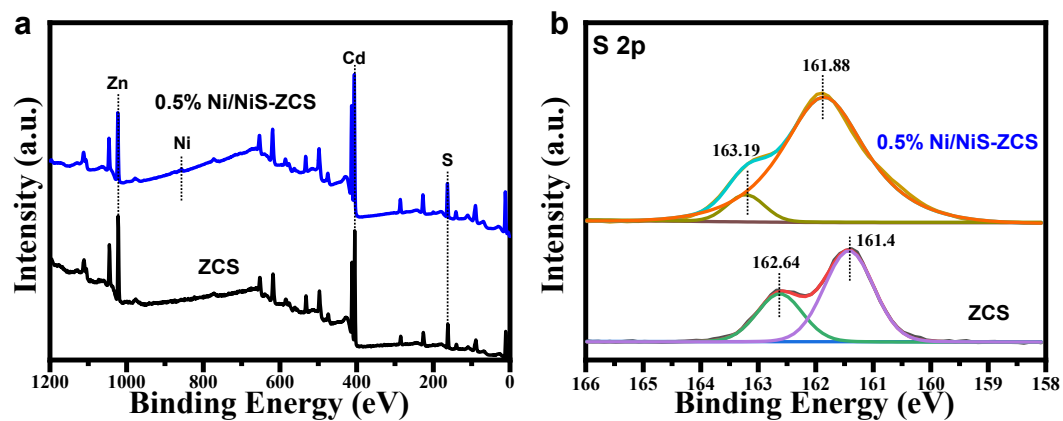


Fig. S3. XRD patterns of as-prepared NiS sample.



**Fig. S4.** N<sub>2</sub> adsorption-desorption isotherms (inset: the corresponding BET surface area) of ZCS and Ni/NiS-ZCS samples.



**Fig. S5.** (a) XPS full spectra survey and (b) S 2p XPS spectra of ZCS and 0.5% Ni/NiS-ZCS samples.

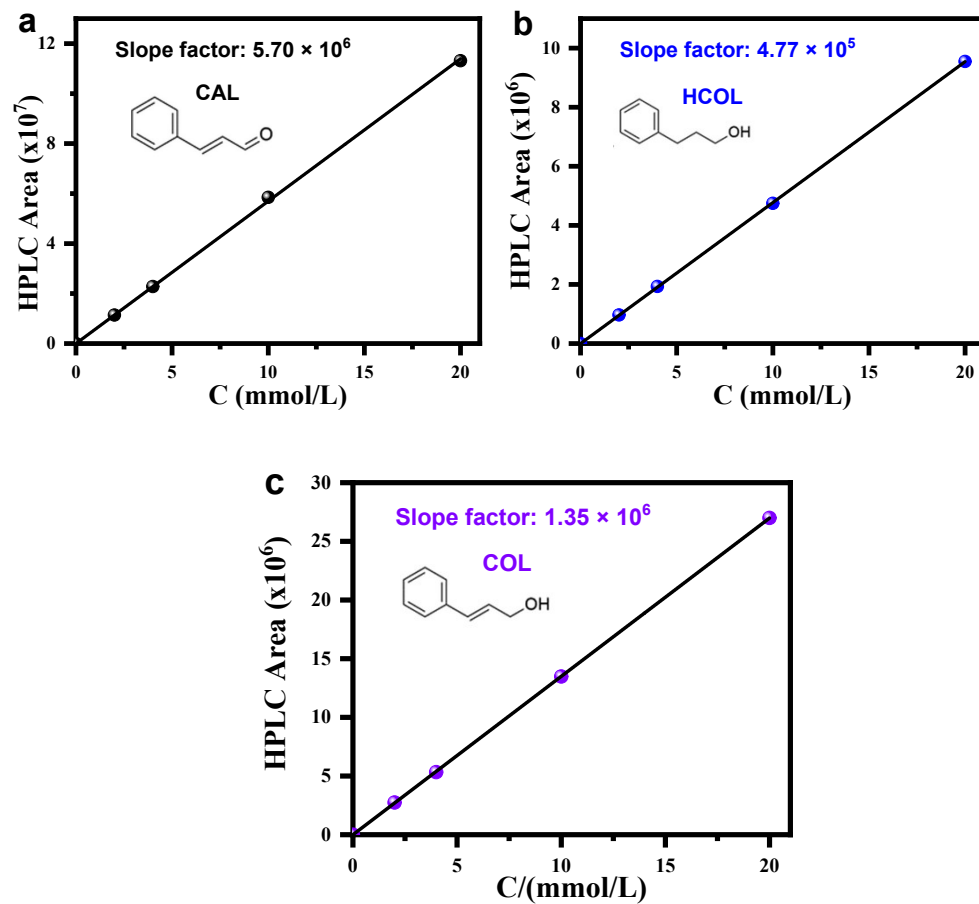


**Fig. S6.** The peak areas for the known product concentrations were used to generate a calibration curve of (a) CAL, (b) HCOL and (c) COL.

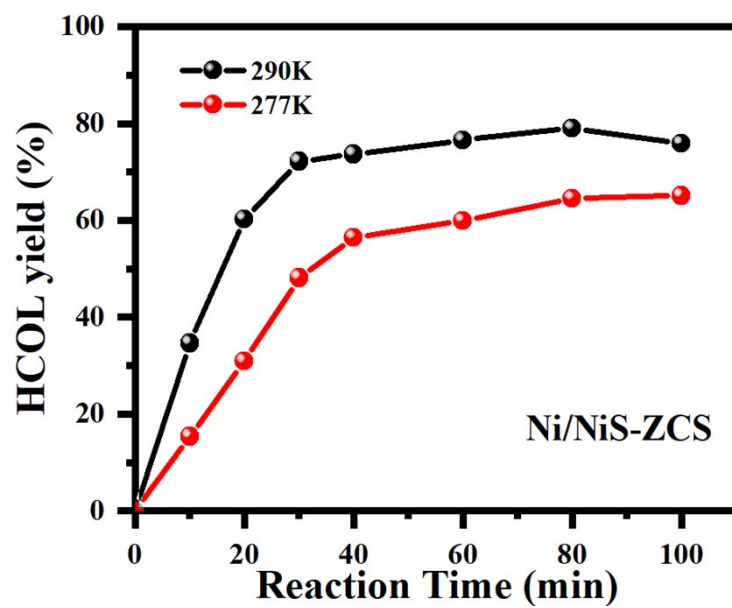


**Fig. S7.** The effect of reaction temperature on the photocatalytic performance upon Ni/NiS-ZCS sample at two temperatures with 277 K and 290 K.

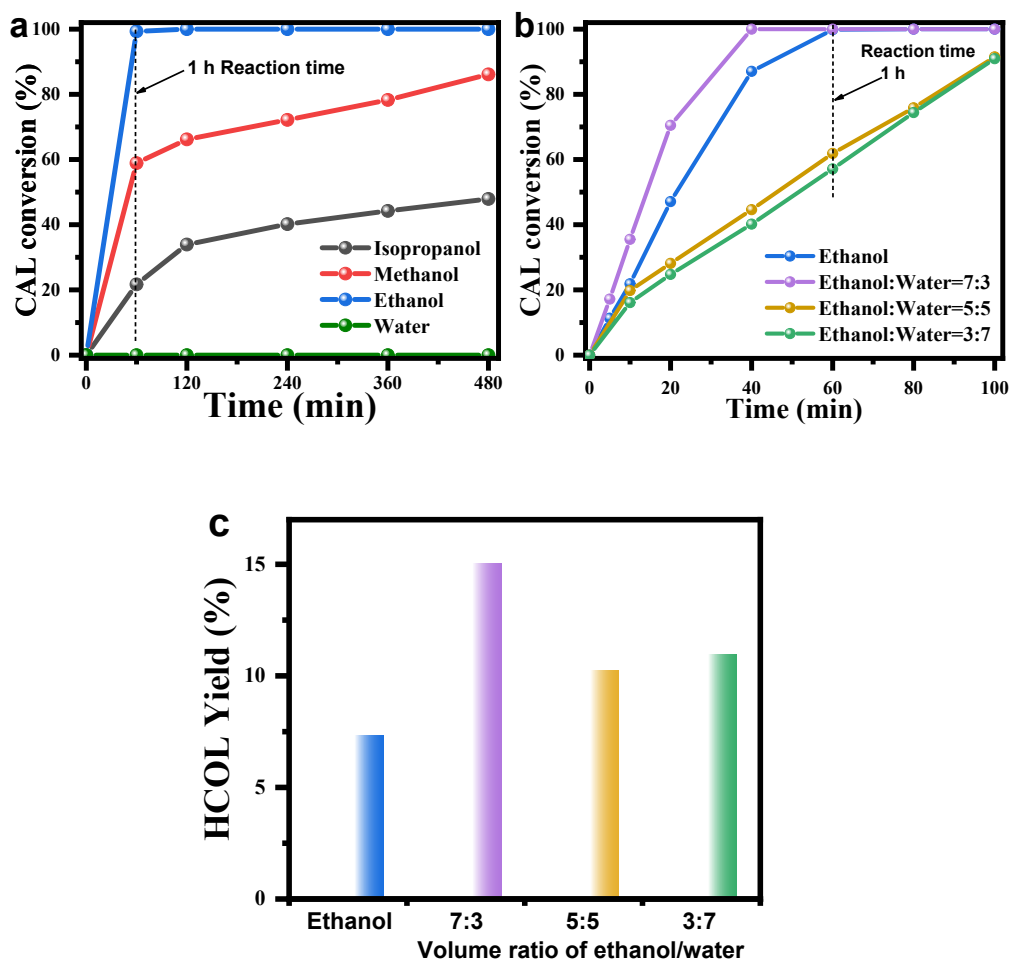


**Fig. S8.** The conversion efficiency of CAL in different (a) solvent composition and (b) volume ratio of ethanol/water system using ZCS as photocatalyst. (c) Bar chart of HCOL yield for 1 h reaction time over ZCS photocatalyst.



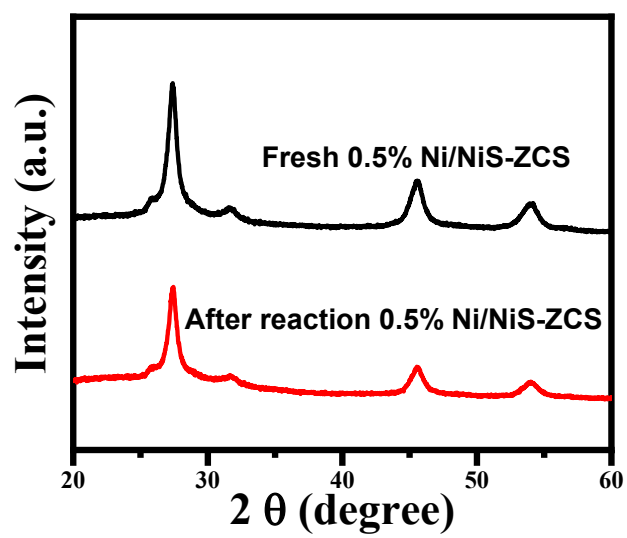


**Fig. S9.** XRD patterns of fresh and used 0.5% Ni/NiS-ZCS samples.

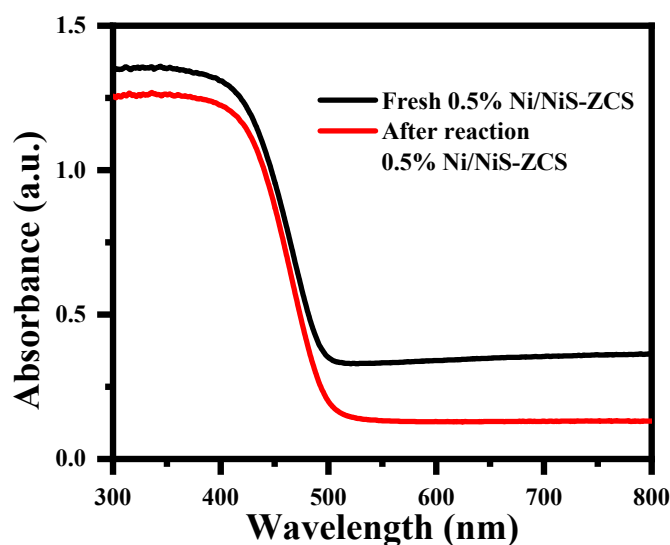


**Fig. S10.** UV-vis spectra of fresh and used 0.5% Ni/NiS-ZCS samples.

**Note:** The optical characterization of used 0.5% Ni/NiS-ZCS in Fig. S10 shows a little inferior absorption capacity than the fresh sample. According to the ICP result (Table S6), it shows that the supernatant liquid of reacted system contains a small number of  $\text{Ni}^{2+}$  and  $\text{S}^{2-}$ . These ions should come from the slight dissolution of Ni/NiS nanoparticle on the surface of catalyst during the photocatalytic reaction process. The slight loss of  $\text{Ni}^{2+}$  and  $\text{S}^{2-}$  results in the inferior absorption in the range of 550-800 nm. Considering the fact that the Ni/NiS-ZCS sample was prepared in the presence of  $\text{S}^{2-}$  solution under light irradiation, it is inevitable that Ni/NiS-ZCS sample dispersed in the water-ethanol reaction solution maintains the ion solubility equilibrium. Although the long-time test of Ni/NiS-ZCS sample displays stable reaction activity (Fig. 3c) and the structural and chemical property (Fig. S9 and S11) remain unchanged, it is admitted that the slight loss of  $\text{Ni}^{2+}$  and  $\text{S}^{2-}$  has a negative effect on the improvement of photocatalytic activity. In the following work, the preparation method should be further optimized to ensure the prepared catalyst with minimizing the ion loss and achieving high activity.

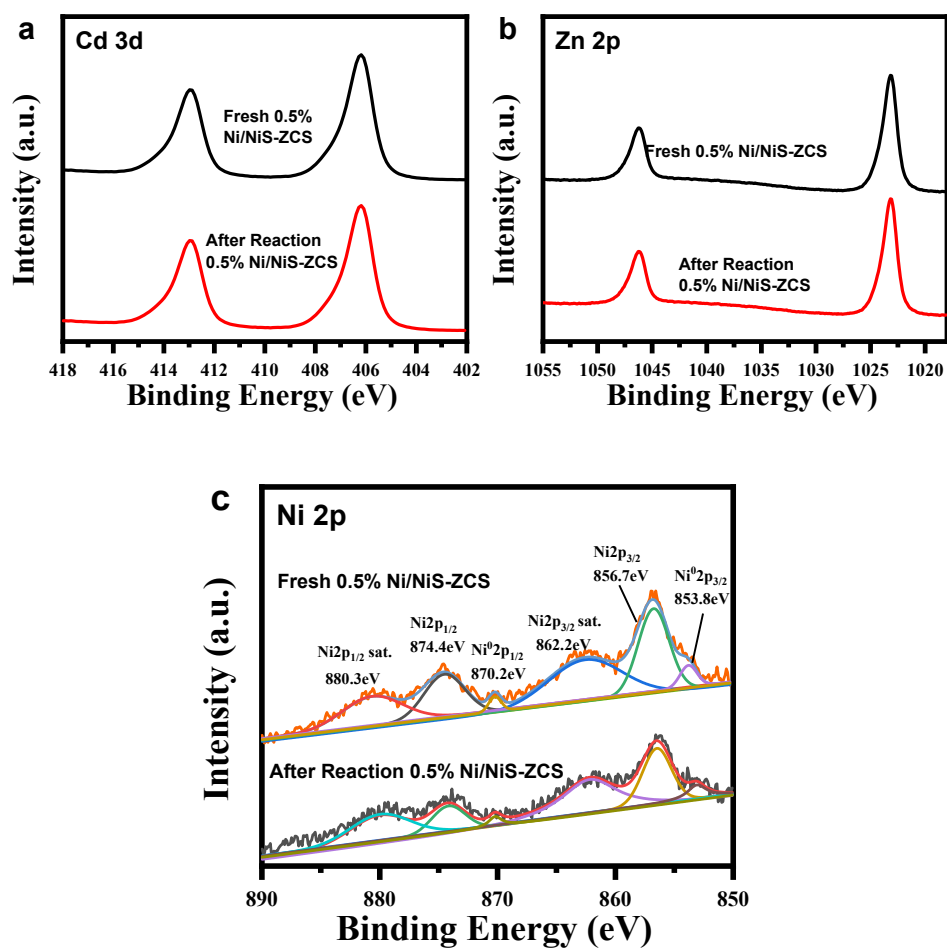


**Fig. S11.** (a) Cd 3d, (b) Zn 2p and (c) Ni 2p XPS spectra of fresh and used 0.5% Ni/NiS-ZCS samples.

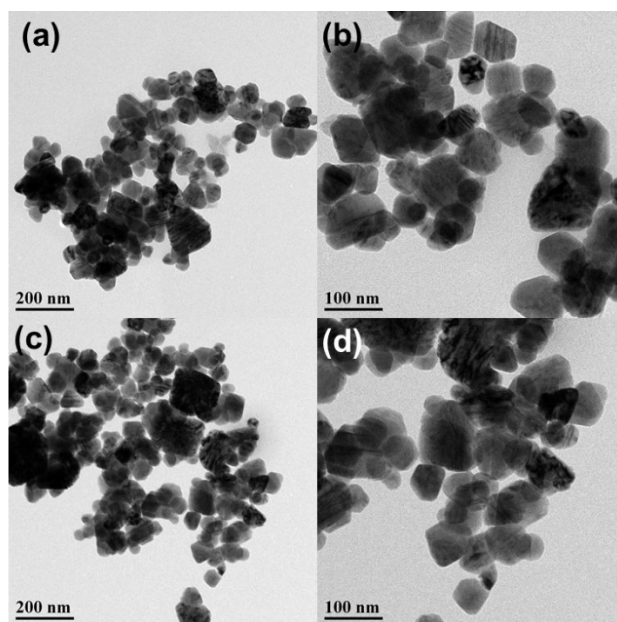


**Fig. S12.** TEM images of fresh and used 0.5% Ni/NiS-ZCS samples.

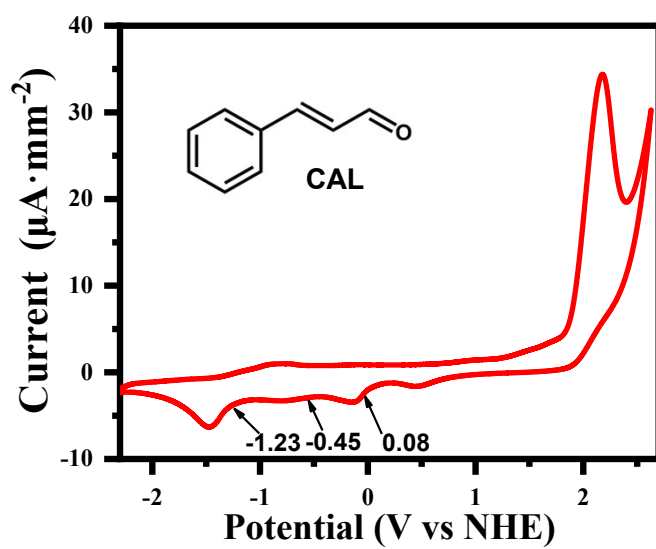
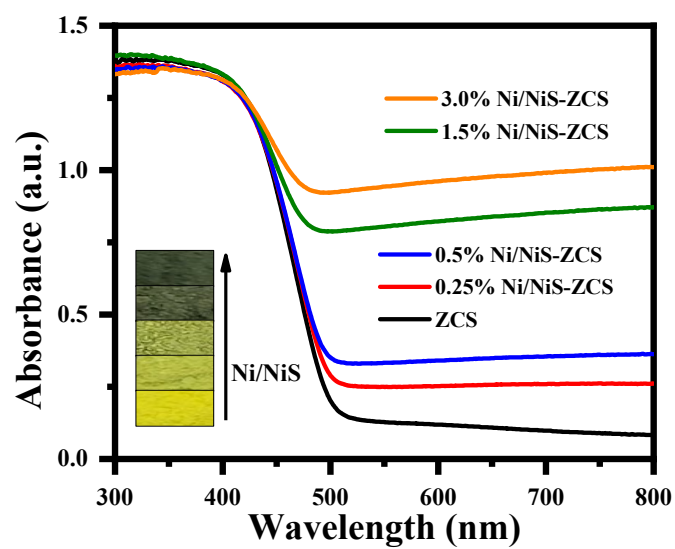
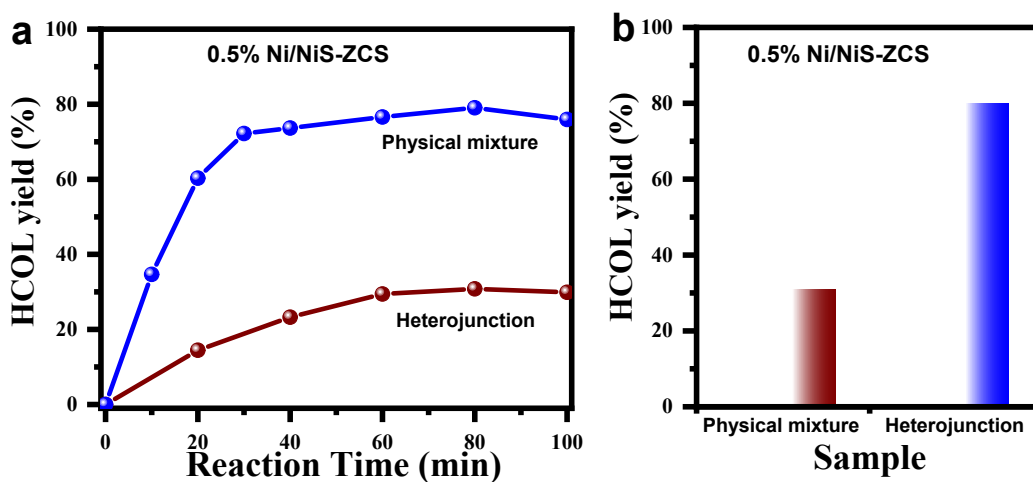


Fig. S13. The cyclic voltammety of CAL.



**Fig. S14.** UV-Vis diffuse reflectance spectra of ZCS and Ni/NiS-ZCS samples.



**Fig. S15.** (a) HCOL yield with the reaction time for Ni/NiS-ZCS and NiS-ZCS Mix samples. (b) Bar chart of HCOL yield for 1 h reaction time over Ni/NiS-ZCS and NiS-ZCS Mix samples.

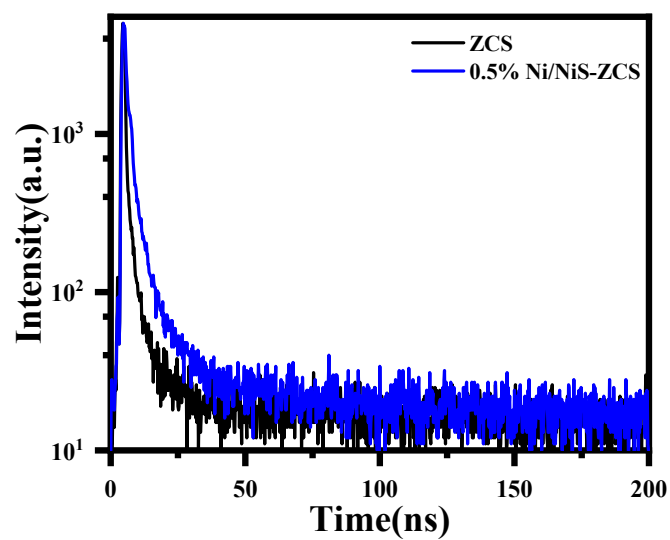


**Fig. S16.** Fluorescence lifetime of ZCS and 0.5% Ni/NiS-ZCS samples.



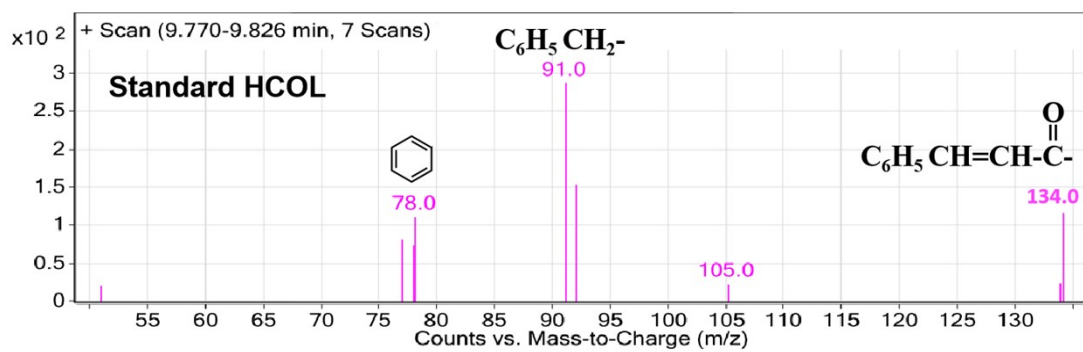


**Fig. S17.** Mass spectra of standard HCOL in ethanol-water (7:3) solvent.

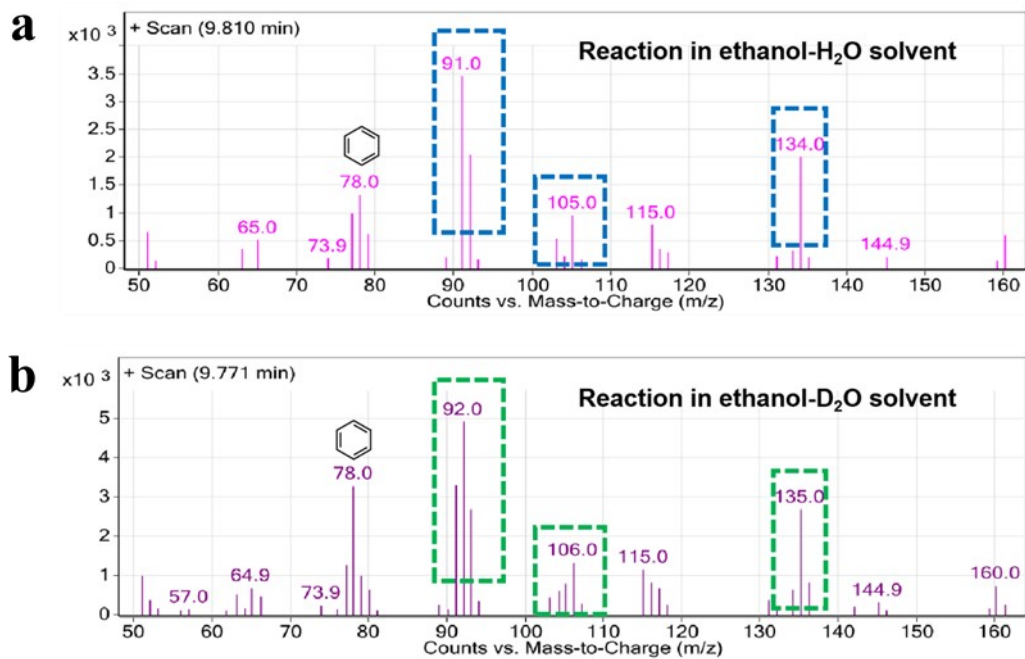


**Fig. S18.** Mass spectrometry test results of reaction products under (a) ethanol-water and (b) ethanol-D<sub>2</sub>O solvent.

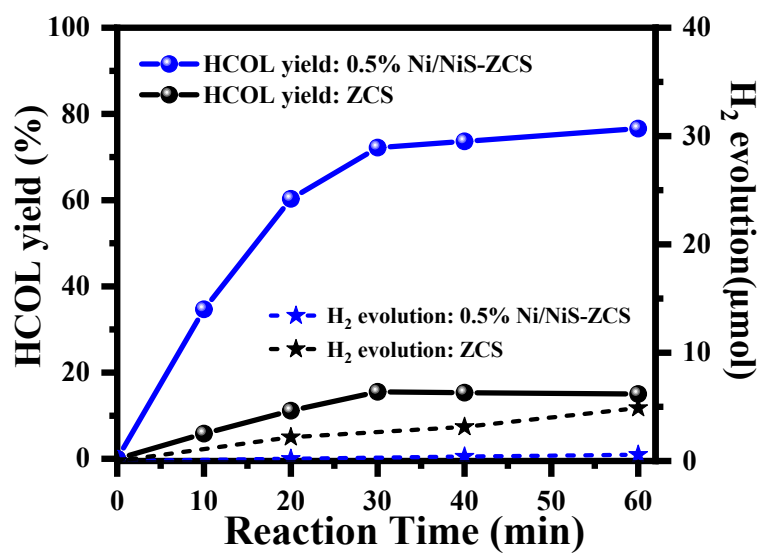


**Fig. S19.** Photocatalytic activity of hydrogen evolution and HCOL yield with 0.5% Ni/NiS-ZCS (20 mg) photocatalyst under visible light irradiation.

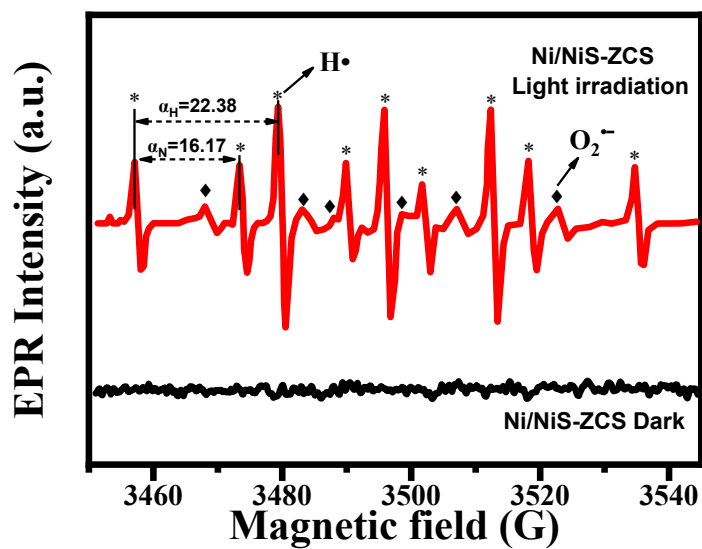


**Fig. S20.** Liquid-phase EPR spin-trapping experiment containing Ni/NiS-ZCS photocatalyst, ethanol/H<sub>2</sub>O solvent, CAL reactant, and DMPO radical trapping agent in air.

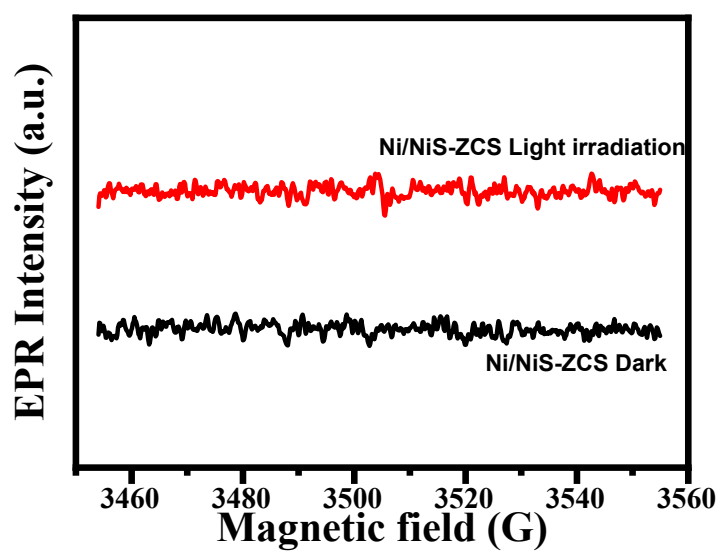


**Fig. S21.** EPR spectra of DMPO-•OH adducts containing Ni/NiS-ZCS photocatalyst, CAL reactant, and DMPO radical trapping agent in N<sub>2</sub> atmosphere.

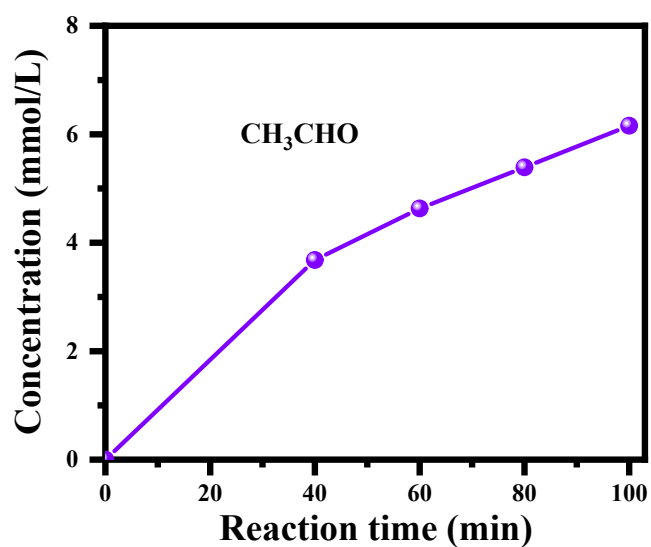


**Fig. S22.** Results of acetaldehyde detection in HPLC.

Detection method of acetaldehyde :

Use 2,4-dinitrophenylhydrazine (DNPH) in acetonitrile as a derivatizing agent, derivatize in a water bath at 333 K for 30 minutes, add cyclohexane for extraction, and test HPLC. The HPLC conditions are in the Fig. S15: the mobile phase is acetonitrile, water=6:4, the injection volume is  $1\mu\text{L}$ , the detection wavelength is 365 nm, the column temperature is 313 K, and the flow rate is 1 mL/min.

**Table S1.** The corresponding atomic content of different catalysts based on ICP-AES.

<b>Catalysts</b>	<b>The atomic content (%)</b>			
	<b>Zn</b>	<b>Cd</b>	<b>Ni</b>	<b>S</b>
ZCS	25.08	24.47	/	50.45
0.25% Ni/NiS-ZCS	24.52	24.64	0.24	50.60
0.5% Ni/NiS-ZCS	23.75	24.62	0.39	51.24
1.5% Ni/NiS-ZCS	22.23	23.20	1.41	53.16
3.0% Ni/NiS-ZCS	22.02	23.12	2.73	52.13

**Table S2.** Photocatalytic reduction of CAL to HCOL under different solvent composition.<sup>a</sup>

<b>Catalysts</b>	<b>solvents</b>	<b>Conversion of CAL (%)</b>	<b>Yield of HCOL (%)</b>
ZCS	Isopropanol	21.71	0.95
ZCS	Methanol	58.88	0.51
ZCS	Ethanol	99.32	7.31
ZCS	Water	0	/
ZCS	Ethanol: Water=9:1	94.20	11.34
ZCS	Ethanol: Water=7:3	100	15.02
ZCS	Ethanol: Water=5:5	61.88	10.23
ZCS	Ethanol: Water=3:7	57.13	10.98
ZCS	Ethanol: Water=1:9	31.30	5.59
0.25% Ni/NiS-ZCS	Ethanol: Water=7:3	100	57.15
0.5% Ni/NiS-ZCS	Ethanol: Water=7:3	100	76.59
1.5% Ni/NiS-ZCS	Ethanol: Water=7:3	100	51.07
3% Ni/NiS-ZCS	Ethanol: Water=7:3	100	48.92

<sup>a</sup> Reaction conditions: 20 mg photocatayst, 0.1 mmol Cinnamaldehyde, total 1 hour reaction time; reaction mixtures were determined by HPLC.



**Table S3.** Summary of photocatalysts reported for CAL reduction.

catalyst	CAL concentration (mmol)	amount of catalyst	T (K)	P <sub>H<sub>2</sub></sub> (bar)	t (h)	solvent	conv. (%)	selec. HCOL (%)
Ni/TiO <sub>2</sub> -HH <sup>[2]</sup>	1.2g	150mg	393	20	1	methanol	99	21.3
Ni/TiO <sub>2</sub> -DP <sup>[2]</sup>	1.2g	150mg	393	20	1	methanol	70	5.3
NiIr <sub>4</sub> <sup>[3]</sup>	0.13mol	30mg	353	10	3	methanol	83	2
Ni-Co/AC <sup>[4]</sup>	20ml	0.5g	423	5	9.5	ethanol	63.2	2.6
Ru/CNTs(a) <sup>[5]</sup>	2mmol	10mg	343	10	10.3	2-propanol	40	8
Ru/TEGO(a) <sup>[6]</sup>	2mmol	10mg	343	10	2.7	2-propanol	40	8
Au-PVP/SiO <sub>2</sub> <sup>[7]</sup>	4mmol	50mg	423	20	4	xylene	18	4
Ir/GA <sup>[8]</sup>	2ml	0.1g	343	20	1	2-propanol	85.8	6.6
Pd-NMC <sup>[9]</sup>	4mmol	25mg	303	5	3	acetonitrile	71.2	11.7
Pd-NMC <sup>[9]</sup>	4mmol	25mg	303	5	3	2-propanol	100	4.9
Pd-NMC <sup>[9]</sup>	4mmol	25mg	303	5	3	toluene	57.3	12.5
Pd-NMC <sup>[9]</sup>	4mmol	25mg	303	5	3	H <sub>2</sub> O	23.2	18.8
Pd/BP <sup>[10]</sup>	0.3mmol	32.8mg	298	1	8	ethanol	100	8
Pd@TNT <sup>[11]</sup>	0.2g	20mg	303	5	7	hexane	100	12
Pd/Fe <sub>3</sub> O <sub>4</sub> @C <sup>[12]</sup>	2ml	38mg	353	14	10	ethanol	100	29
PtFe <sub>0.25</sub> /15AS <sup>[13]</sup>	7.5mmol	50mg	363	20	0.5	2-propanol	77.4	7.8
Pt/15TS <sup>[14]</sup>	7.5mmol	50mg	363	40	1	2-propanol + H <sub>2</sub> O	90	17.6
Pt-FeO <sub>x</sub> /15TS-773 <sup>[14]</sup>	7.5mmol	50mg	363	20	0.5	2-propanol + H <sub>2</sub> O	68	3.9
Pt <sub>3</sub> Ni@Ni <sub>32</sub> Cu(OH) <sub>2</sub> <sup>[15]</sup>	0.8mmol	1mg	323	30	3	ethanol	98.5	7.6
Pt/YCo <sub>0.3</sub> Fe <sub>0.7</sub> O <sub>3</sub> <sup>[16]</sup>	0.5g	25mg	363	20	0.5	2-propanol + water	98.9	4.6
<b>This work</b>	<b>0.1mmol</b>	<b>20mg</b>	<b>R.T.</b>	<b>0</b>	<b>1</b>	<b>ethanol + water</b>	<b>100</b>	<b>80</b>

**Table S4.** The absolute fluorescence quantum yield (%) and fluorescence lifetime of samples excited at 380 nm in the wavelength range of 400-750 nm.

<b>Photocatalyst</b>	<b>fluorescence lifetime (ns)</b>	<b>Absolute fluorescence quantum yield (%)</b>
ZCS	1.35	5.50
0.5% Ni/NiS-ZCS	5.14	0.96
1.5% Ni/NiS-ZCS	2.83	1.05

**Table S5.** Black experiments without catalyst nor light irradiation. <sup>a</sup>

<b>Entry</b>	<b>Photocatalyst</b>	<b>Irradiation condition</b>	<b>CAL conversion (%)<sup>c</sup></b>	<b>HCOL yield (%)<sup>d</sup></b>
1	0.5% Ni/NiS-ZCS	/	/	/
2	/	> 420 nm	/	/

<sup>a</sup> Reaction conditions: 20 mg 0.5% Ni/NiS-ZCS, 0.1 mmol Cinnamaldehyde, total 2-hour reaction time; reaction mixtures were determined by HPLC.

**Table S6.** ICP results of the supernatant after centrifugation of the catalyst in the system before and after the reaction.

<b>Samples</b>	<b>The elements content (mg/kg)</b>	
	<b>Ni</b>	<b>S</b>
<b>Before reaction</b>	/	/
<b>After reaction</b>	0.85	8.02

## Reference

- [1] Guo X, Guo P, Wang C, et al. Few-layer WSe<sub>2</sub> nanosheets as an efficient cocatalyst for improved photocatalytic hydrogen evolution over Zn<sub>0.1</sub>Cd<sub>0.9</sub>S nanorods[J]. *Chemical Engineering Journal*, 2020, **383**: 123183.
- [2] Prakash M G, Mahalakshmy R, Krishnamurthy K R, et al. Selective hydrogenation of cinnamaldehyde on nickel nanoparticles supported on titania: Role of catalyst preparation methods[J]. *Catalysis Science & Technology*, 2015, **5**: 3313-3321.
- [3] Feldmann C, Egeberg A, Dietrich C D, et al. Bimetallic NiIr<sub>4</sub> and NiOS<sub>4</sub> alloy nanoparticles and their catalytic performance in hydrogenation reactions[J]. *ChemCatChem*, 2017, **9**: 3534-3543.
- [4] Malobela L J, Heveling J, Augustyn W G, et al. Nickel–cobalt on carbonaceous supports for the selective catalytic hydrogenation of cinnamaldehyde[J]. *Industrial & Engineering Chemistry Research*, 2014, **53**: 13910-13919.
- [5] Wang Y, Rong Z, Wang Y, et al. Ruthenium nanoparticles loaded on multiwalled carbon nanotubes for liquid-phase hydrogenation of fine chemicals: An exploration of confinement effect[J]. *Journal of Catalysis*, 2015, **329**: 95-106.
- [6] Wang Y, Rong Z, Wang Y, et al. Ruthenium nanoparticles loaded on functionalized graphene for liquid-phase hydrogenation of fine chemicals: Comparison with carbon nanotube[J]. *Journal of Catalysis*, 2016, **333**: 8-16.
- [7] Zhong R Y, Sun K, Hong Y-C, et al. Impacts of organic stabilizers on catalysis of Au nanoparticles from colloidal preparation[J]. *ACS Catalysis*, 2014, **4**: 3982-3993.
- [8] Li L, Gao G, Zheng J, et al. Three-dimensional graphene aerogel supported Ir

nanocomposite as a highly efficient catalyst for chemoselective cinnamaldehyde hydrogenation[J]. *Diamond and Related Materials*, 2019, **91**: 272-282.

[9] Nagpure A S, Gurralla L, Gogoi P, et al. Hydrogenation of cinnamaldehyde to hydrocinnamaldehyde over Pd nanoparticles deposited on nitrogen-doped mesoporous carbon[J]. *RSC Advances*, 2016, **6**: 44333-44340.

[10] Fujiwara S, Takanashi N, Nishiyabu R, et al. Boronate microparticle-supported nano-palladium and nano-gold catalysts for chemoselective hydrogenation of cinnamaldehyde in environmentally preferable solvents [J]. *Green Chemistry*, 2014, **16**: 3230-3236.

[11] Yang X, Wu L, Ma L, et al. Pd nano-particles (NPs) confined in titanate nanotubes (TNTs) for hydrogenation of cinnamaldehyde [J]. *Catalysis Communications*, 2015, **59**: 184-188.

[12] Jianyan Yu, Li Yan, Gaomei Tu, et al. Magnetically responsive core-shell Pd/Fe<sub>3</sub>O<sub>4</sub>@C composite catalysts for the hydrogenation of cinnamaldehyde [J]. *Catalysis Letters*, 2014, **144**: 2065-2070.

[13] Pan H, Li J, Lu J, et al. Selective hydrogenation of cinnamaldehyde with PtFe<sub>x</sub>/Al<sub>2</sub>O<sub>3</sub>@SBA-15 catalyst: Enhancement in activity and selectivity to unsaturated alcohol by Pt-FeO<sub>x</sub> and Pt-Al<sub>2</sub>O<sub>3</sub>@SBA-15 interaction[J]. *Journal of Catalysis*, 2017, **354**: 24-36.

[14] Xue Y, Yao R, Li J, et al. Efficient Pt-FeO<sub>x</sub>/TiO<sub>2</sub>@SBA-15 catalysts for selective hydrogenation of cinnamaldehyde to cinnamyl alcohol[J]. *Catalysis Science & Technology*, 2017, **7**: 6112-6123.

[15] Wang P, Shao Q, Cui X, et al. Hydroxide-membrane-coated Pt<sub>3</sub>Ni nanowires as highly efficient catalysts for selective hydrogenation reaction[J]. *Advanced Functional Materials*, 2018, **28**: 1705918.

[16] Xue Y, Xin H, Xie W, et al. Pt nanoparticles supported on YCo<sub>x</sub>Fe<sub>1-x</sub>O<sub>3</sub> perovskite oxides: Highly efficient catalysts for liquid-phase hydrogenation of cinnamaldehyde[J]. *Chemical Communications*, 2019, **55**: 3363-3366.